Research Article

Na Ning, Yiping Qiu, and Yi Wei*

Building effective core/shell polymer nanoparticles for epoxy composite toughening based on Hansen solubility parameters

https://doi.org/10.1515/ntrev-2021-0077
received June 18, 2021; accepted August 28, 2021

Abstract: Particles have been demonstrated to toughen epoxy resins, especially for fiber-reinforced epoxy composites, and core/shell particles are one of them. It is known that not all particles toughen the same but most evaluations are through experimentation, and few studies have been conducted to accurately predict the particles' toughening effect or guide the design of effective particles. In this study, efforts were made to find the control factors of core/shell particles, primarily interfacial compatibility and degree of dispersion, and how to predict them. Nanocomposites were fabricated by incorporating core/shell nanoparticles having various shell polymer compositions, especially their polarities. Their compatibility was estimated using a novel quantitative approach *via* adopting the theory of Hansen solubility parameters (HSP), in which the HSP of core/shell nanoparticles and the epoxy matrix were experimentally determined and compared. It was found that the HSP distance was a good predictor for particle dispersion and interfacial interaction. Particles having a small HSP distance (R_a) to the epoxy resin, represented by the polybutylacrylate core/polymethyl methacrylate shell particle having the smallest R_a of 0.50, indicated a uniform dispersion and strong interfacial bonding with the matrix and yielded outstanding toughening performance. In contrast, polybutylacrylate core/polyacrylonitrile shell particle having the largest HSP distance (6.56) formed aggregates and exhibited low interfacial interaction, leading to poor toughness. It was also demonstrated that HSP can provide an effective strategy to facilitate the design of effective core/shell nanoparticles for epoxy toughening.

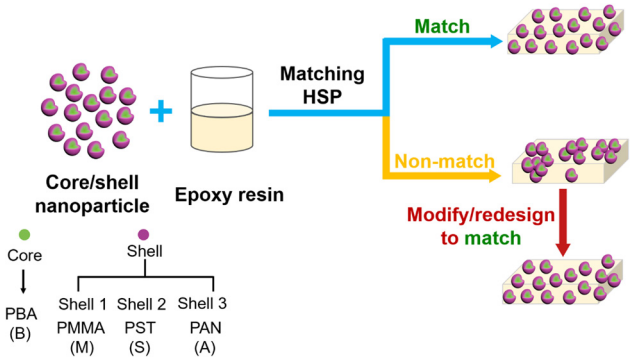

Graphical abstract

Keywords: core/shell nanoparticles, epoxy resins, HSP, fracture toughness, dispersion, interfacial interaction

1 Introduction

Epoxy resins are one of the most important thermoset polymers in composites. As thermosetting materials, epoxies exhibit a high degree of crosslinking, which endows them high rigidity and strength [1]. However, the highly crosslinked structure also makes epoxies inherently brittle, which consequently suffered poor crack resistance characterized by the low fracture toughness [2,3]. For decades, research on toughening the brittle epoxy resins has been active in both academia and industry. A major strategy to improve their fracture toughness is the incorporation of fillers, either soft or rigid, organic or inorganic. However, in most cases, these fillers are unsatisfactory because there is a trade-off between toughness and other important mechanical properties, such

* **Corresponding author: Yi Wei,** Center for Civil Aviation Composites, Donghua University, 2999 North Renmin Road, Shanghai, 201620, China; Key Laboratory of Textile Science & Technology, Ministry of Education, College of Textiles, Donghua University, 2999 North Renmin Road, Shanghai, 201620, China, e-mail: weiy@dhu.edu.cn
Na Ning: Center for Civil Aviation Composites, Donghua University, 2999 North Renmin Road, Shanghai, 201620, China; Key Laboratory of Textile Science & Technology, Ministry of Education, College of Textiles, Donghua University, 2999 North Renmin Road, Shanghai, 201620, China
Yiping Qiu: Key Laboratory of Textile Science & Technology, Ministry of Education, College of Textiles, Donghua University, 2999 North Renmin Road, Shanghai, 201620, China

as strength, modulus, and glass transition temperature (T_g) [4]. In principle, as a measure for property balances, adding fillers containing soft and rigid phases into epoxy resin will improve its toughness without significantly affecting mechanical properties [5–7], wherein core/shell particles were proven effective tougheners for brittle epoxy resin [8–10]. Although core/shell particles can increase the fracture toughness of epoxy matrix without significantly lowering other mechanical properties, previous work is more inclined to focus on the effect of particle size and particle loading, and there are almost no established particle design guidelines, and the theoretical explanation of toughening mechanism involving these particles is missing. In this work, by carefully controlling the composition and morphology of nanoparticles, a credible theory is proposed for the first time to quantitatively explain and predict the toughening effect and the performance of core/shell nanoparticles.

Rubber particles are the most commonly used and effective toughening additive for brittle epoxy resins, whether they are amorphous or semi-crystalline [11,12], thermosets or thermoplastics [13,14]. Nonetheless, the toughness improvement usually comes at the expense of a reduction in strength, modulus, and T_g because of the low modulus of rubber particles [15,16]. Rigid particles, such as silica [17], carbon nanotubes [18,19], carbon nanofibers [20,21], and graphene and its derivates [22,23] are also used as tougheners for brittle epoxy resin due to low reductions in modulus and strength. However, these rigid fillers often do not impart significant toughness improvement.

Fillers containing soft and rigid phases prove effective to boost the toughness of epoxy resins with a low reduction in strength and modulus [4,24]. Core/shell polymer particles, a type of structured composite material, formed by at least two substances of different chemical composites, are considered as an ideal candidate as toughening agent [25]. Jiang *et al.* reported that simultaneous reinforcing and toughening effect could be obtained by adjusting the loading of core/shell particles and the ratio between the shell thickness and core diameter [8]. It was also demonstrated in an earlier publication that the critical stress intensity factor (K_{IC}) of epoxy resins increased by 220% *via* incorporation of soft poly (butyl acrylate) core and rigid poly(methyl methacrylate) shell nanoparticles [26].

The toughening efficiency of nanofillers depends heavily on their dispersion states and interfacial interaction between nanofillers and resin matrix [27–29], and core/shell particles are no exception. A well-dispersed filler in the epoxy matrix is a prerequisite for epoxy toughening, and strong filler–matrix interfacial interaction facilitates effective stress transfer between the two phases [30,31].

Good dispersion and strong interfacial interaction both require high surface compatibility between the filler and epoxy matrix [32]. The most commonly used method to improve the compatibility between a filler and the epoxy matrix is to introduce the filler surface with functional groups [32,33]. Literature studies showed that the filler surface modification with amine, carboxylic or epoxide groups not only improves the dispersion of filler in an epoxy matrix but also enhances the interfacial stress transfer between the filler and epoxy matrix through interfacial reactions induced by these surface-reactive groups [27,30].

However, a few studies have been conducted to explore the relationship among particle compositions, morphologies and the compatibility of epoxy resin from the perspective of particle design. In addition, to the best of our knowledge, most studies on epoxy toughening with core/shell particles were from the perspective of particle sizes or particle loading levels, and there is almost no description of core/shell particle's toughening effect based on its composition, especially based on the shell polymer polarity. Moreover, there is a clear absence of theories satisfactorily explaining why some particular core/shell particles toughen epoxy resins well, but the others do not, and some of them even significantly lower the toughness.

The design of effective core/shell particles today remains a work of art, even with the commercialization of a few successful products. Researchers rely largely on experience and trial-and-error when it comes to core/shell particle synthesis, which limited the design space and prolonged the development cycle. It becomes essential to establish the design guidelines by building the fundamental understanding of composite performance as a function of particle composition and structure.

Therefore, it was the intention of this work, through careful control of nanoparticle composition and morphology, to obtain important insights into the fundamentals of core/shell nanoparticle toughening, from which credible theories were proposed for the first time to quantitatively explain and predict the toughening performance of core/shell nanoparticles. Three types of nanoparticles with the same core but different shell compositions were prepared. The influence of these three types of core/shell nanoparticles in epoxy resins was investigated by evaluating their dispersion state, rheological and mechanical properties. Furthermore, the Hansen solubility parameters (HSP) of the formulated epoxy resin and the shell compositions were measured experimentally and were used to

quantitatively describe the compatibility between core/shell nanoparticles and the epoxy matrix. The results not only showed that the performances of the core/shell nanoparticles in the epoxy matrix were greatly affected by the polarity of the shell polymer but also demonstrated good quantitative agreement with compatibility predictions based on the HSP theory. It is further illustrated that nanoparticles used for epoxy resin toughening could be designed or modified under the guidance of the HSP theory.

2 Experimental

2.1 Materials

Butyl acrylate (BA, 99%), methyl methacrylate (MMA, 99.5%), styrene (ST, 99%), acrylonitrile (AN, 99%), glycidyl methacrylate (GMA, 97%) and ethylene glycol dimethacrylate (EGDMA, 98%) were purchased from Sigma Aldrich and used without further purification. Sodium 4-dodecylbenzenesulfonate (SDBS, 88%) and sodium formaldehyde sulfoxylate solution (SFS, 98%) were supplied by Adamas and Macklin, respectively. Ammonium persulfate (APS, 98%) and 2-butanone (MEK, 99%) were purchased from Sinopharm. E828, a type of diglycidyl ether of bisphenol-A epoxy (DGEBA) with an epoxy equivalent weight (EEW) of 185 was supplied by Sanmu Group Co, Ltd. Neopentyl glycol diglycidyl ether (NGDGE, EEW 137) was supplied by Huite Chemical, Ltd. 2-Ethyl-4-methylimidazole (2E4MI) and methyl hexahydrophthalic anhydride (MHHPA, 98%) were purchased from Yuancheng Sichuang Technology Co. Ltd. and J&K Chemicals Inc, respectively.

2.2 Preparation of core/shell nanoparticles

Formulations for nanoparticle synthesis are given in Table S1 (Supplementary Information). A particle with a soft polymer core and a hard polymer shell was selected as the core/shell configuration because it provided the largest toughness improvement, based on the published work [26]. For the precise control of the particle composition, all core/shell particles were synthesized with the same soft core and different rigid shells *via* a two-stage polymerization. Furthermore, to minimize the effect of varying T_g of the shell composition, three polymers having almost the same T_g while exhibiting significant differences in polarity were selected to construct the shell, namely polymethyl methacrylate (PMMA, designated as M), polystyrene (PST, designated as S) and polyacrylonitrile (PAN, designated as A). The resulting core/shell structures were denoted B/M, B/A, B/S, wherein B was the poly(butyl acrylate) core and M was the poly(methyl methacrylate) shell, and so on. The B/S particles that were surface-modified with GMA at different loading levels were named B/S-5, B/S-10 and B/S-15, wherein the number denoted the percentage of the functional monomer GMA in the shell polymer composition. The synthesis method and procedure were the same as reported in a previous study [26].

2.3 Epoxy composites fabrication

In order to maintain the particle morphology, the core/shell nanoparticles were re-dispersed in the epoxy resin using a phase-transfer method, described in an earlier publication [26]. The epoxy resins were mixed with the anhydride hardener, with a 1:1 stoichiometric ratio of epoxy groups/anhydride groups. For all samples, the loadings of core/shell particles and cure accelerator (2E4MI) were kept at 10 and 0.5 wt%, respectively. The resin mixture was poured into aluminum molds with specific dimensions and degassed for 1 h at 60°C. All the particles were incorporated into the same resin formula and cured under the same profile, which was 120°C for 1 h, plus 140°C for 2 h and finally 170°C for 1 h.

2.4 Determination of HSP

HSP of core/shell particles and epoxy matrix were determined based on the observation of the interaction between the material and solvents [32,34]. In the case of formulated epoxy resins, 0.5 g of the resin was added into 18 different solvents with known HSP and dwelled for 24 h. The mixture was rated either as “1” or “0”, based on the observation of the dispersion state of epoxy resins in the solvent. A rating of “1” represented a resin being fully dissolved in that particular solvent, while a rating of “0” denoting a resin that was insoluble. Due to the crosslinked structure and particulate form of the core/shell particles, they were dried into films and the film’s degree of swelling was used for the rating. For higher precisions, the degree of swelling was rated according to six grades. A rating of “5” designated the highest degree of swelling in a particular solvent. A rating of “0” denoted no swelling or minimal degree of swelling. It was important that the particles be

completely dried at a temperature higher than their minimum film formation temperature (MFFT), so that a film, instead of powder, could be obtained. However, by experimentally determining the degree of swelling for core/shell particles, two assumptions were made: (1) the synthesized core/shell particle had a perfect core/shell structure, that is, the core layer polymer was completely wrapped in the shell layer polymer, and (2) the swelling of core/shell particles was only related to the shell polymer and the contribution of the core layer polymer was neglected. The ratings for the resin and the core/shell particle film in the selected solvents were processed by HSPiP Software (*Hansen Solubility Parameters in Practice*, 5th Edition), and the HSP components (δ_D, δ_P, and δ_H), and the radius value (R_o) of the sphere of interaction were calculated and fitted.

2.5 Characterization

The particle size and size distribution of the core/shell particles in their original aqueous medium were characterized by dynamic light scattering (DLS) on a Malvern Nano-ZS analyzer. Particle morphology was observed using a JEOL JEM-2100transmission electron microscope (TEM), in which the particles were first stained with phosphotungstic acid (PTA) before subjecting to TEM. Fourier transform infrared (FTIR) spectra were recorded on a Nicolet 6700 FTIR spectrometer using the attenuated total reflection (ATR) mode. The rheological properties of epoxy resins containing core/shell particles were investigated on a TA DHR Rheometer with frequency ramping from 0.1 to 1,000 s^{-1}. The degree of dispersion of core/shell particles in the epoxy matrix was qualitatively characterized by TEM on a thin composite section with the thickness ranging from 30 to 50 nm, which were prepared by freezing-ultramicrotome. Tests on tensile properties and fracture toughness were performed on a Wance ETM104B-EX electronic universal testing machine with a 2 kN load cell, using appropriate fixtures. The dog-bone-shaped tensile samples were prepared according to ASTM D638 and an extensometer was used to measure the strain. Fracture toughness was conducted according to ASTM D5045 using a single-edge-notch bending geometry. A pre-crack was initiated by tapping a sharp chilled blade in the notch. The critical stress intensity factor (K_{IC}) and critical strain energy release rate (G_{IC}) were calculated according to the equations given in ASTM D5045. Each reported value for the tensile and fracture toughness test was the average of at least six specimens. The morphologies of fracture surfaces from tensile tests were coated with gold and inspected on a Hitachi S4800 scanning electron microscope (SEM).

3 Results and discussion

3.1 Core/shell nanoparticle characterization

Three types of nanoparticles with the same core but different shell compositions were prepared *via* emulsion polymerization. The DLS analysis on the particle size and distribution are shown in Figure 1a–c. The Z-average intensity particle diameters (*d*) and polydispersion index (PDI) are presented in Table S2 (Supplementary Information). The particle size distribution curves all had a single peak, indicating that the particles were of monomodal distribution. Moreover, the increase in particle sizes relative to the core composition indicated that the shell monomers were polymerized on top of the cores without new particle nucleation during the second polymerization stage, namely the shell-forming stage.

The synthesized nanoparticles were subjected to TEM to observe their morphologies. The PTA negative staining technique was employed to improve the weak contrast between different polymer phases in the nanoparticles. Figure 1 presents images of B/M (d), B/S (e), and B/A (f) nanoparticles, wherein the light and dark domains corresponded to the core and shell phases, respectively. It is evident from Figure 1(d–f) that the nanoparticles synthesized were spherical with relatively uniform sizes, showing no signs of undesirable secondary particle nucleation.

The particle compositions were verified by FTIR. As shown in Figure 1(h), all three particles exhibited a significant peak at 1,730 cm^{-1}, ascribed to the –C═O stretching vibration ester groups. As expected, the peak in B/A particles at 2,242 cm^{-1} represented the characteristic absorption of –C≡N from PAN. The B/S particles had strong absorptions at 3,027, 1,602, 1,494, 761, and 700 cm^{-1}, which could be attributed to the characteristic bands of –CH and C═C bonds on the benzene ring in PST.

3.2 Dispersion of nanoparticles in epoxy resin

To obtain a uniform epoxy–nanoparticle mixture without compromising its morphology and particle size distribution, the aqueous medium was replaced by an epoxy resin *via* a phase-transfer process, which was a proven technique described in an earlier study [26]. It is worth noting that due to the large difference in the shell polymer polarity of the three types of particles, the actual phase transfer processes might be slightly altered in terms of solvent water ratios. Therefore, it was also necessary to

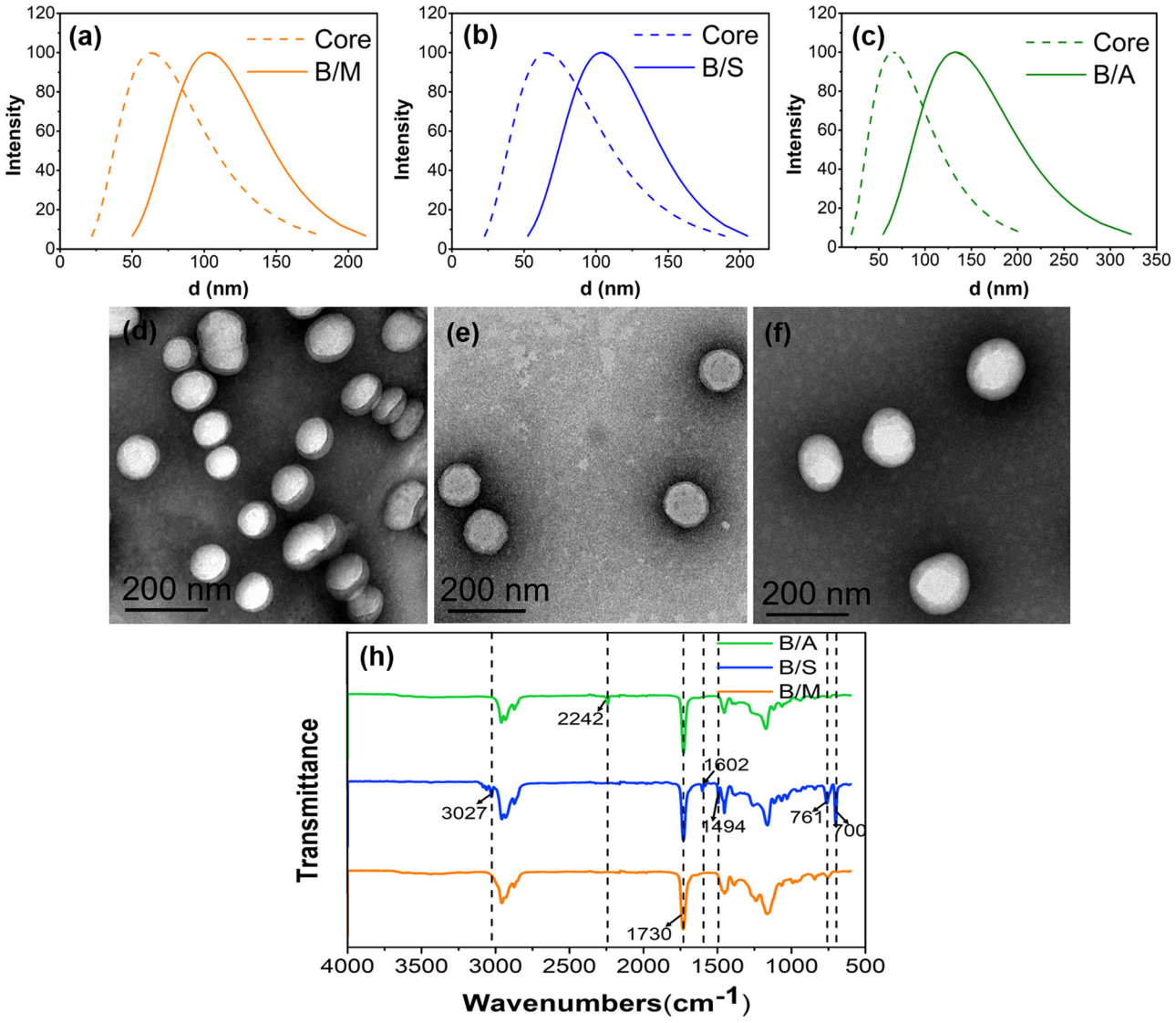

Figure 1: Core/shell nanoparticle characterization. Size distributions: (a) B/M, (b) B/S, (c) B/M. TEM images: (d) B/M, (e) B/S, (f) B/M, and FTIR spectra (h).

verify whether the particle morphology and degree of dispersion were preserved after the phase transfer.

The TEM images of the epoxy resins containing various core/shell nanoparticles are shown in Figure 2. As can be seen the three types of shell polymers, which were significantly different in polarities led to three significantly different particle dispersibility in epoxy resin. The B/M particles in Figure 2(a), having moderate polarity PMMA as the shell polymer, were well dispersed. In contrast, both particles having shell polymers of lower polarity (B/S) and higher polarity (B/A), as shown in Figure 2(b) and (c), exhibited aggregations, with the aggregation of B/A particles to be the most significant.

The degree of nanoparticle dispersion in a resin depends on their mutual compatibility. Since the shell polymer is in contact with the resin, it determines the particles' compatibility with and the degree of dispersion in the epoxy resin. In order to quantitatively characterize, describe and predict the particle compatibility with the epoxy resin, the authors adopted the theory of solubility parameter. According to the principle of "like dissolves like", the solubility of a given polymer in various solvents is largely determined by its chemical structure [35]. Therefore, the HSP are extensively used as a method to quantitatively characterize the structure–property relationship of polymer materials. In addition, HSP are used to predict

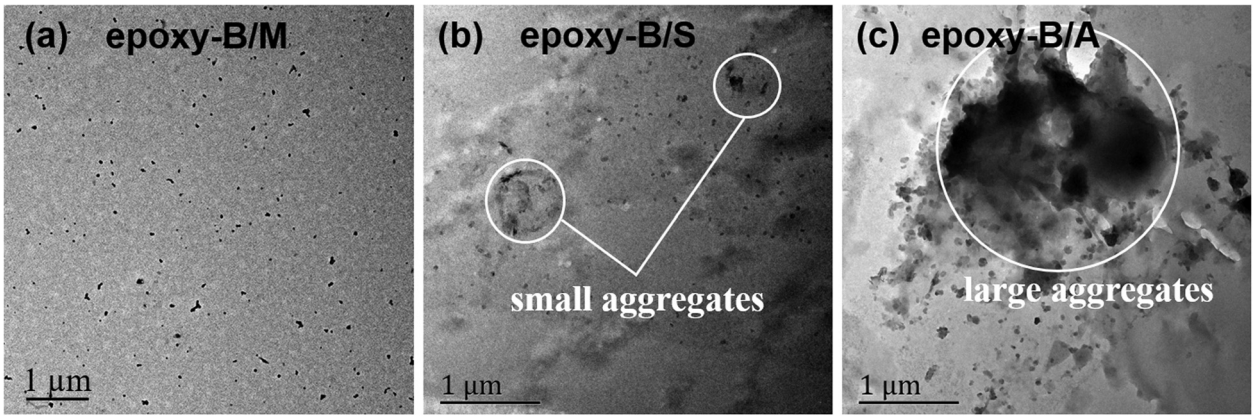

Figure 2: TEM images showing the dispersed nanoparticles in epoxy resin: B/M (a), B/S (b) and B/A (c).

the compatibility of polymers and to characterize the surfaces of fillers to improve their dispersion and adhesion [32,36–38]. Based on a similar principle of "like seeks like," materials with similar HSP values would exhibit high mutual physical affinity or rather compatibility [37]. Thus, a comparison of HSP of the core/shell nanoparticles and the epoxy resin potentially provides insights into the compatibility between them as well as a quantitative view of nanoparticles' degree of dispersion.

The solubility or degree of swelling of a polymer can be measured using a series of solvents with known HSP, and its HSP can be calculated, accordingly, and conveniently by HSPiP. The results are summarized in Table 1, together with the relative energy difference (RED, calculated by HSPiP) values of materials in various solvents. The RED value provides an estimate on whether two materials will be miscible or not, *i.e.*, miscible when RED <1, partially miscible when RED = 1, and immiscible when RED >1 [39,40].

Figure 3 presents the HSP spheres of neat epoxy resin and various core/shell nanoparticles, with each color representing one composition. The HSP values are

Table 1: The rating results and RED values of solubility or swelling of epoxy matrix and core/shell nanoparticles in various solvents with known HSP

Solvent	δ_D (MPa$^{1/2}$)	δ_P (MPa$^{1/2}$)	δ_H (MPa$^{1/2}$)	Neat epoxy		B/M		B/S		B/A	
				R^a	RED	R^b	RED	R^b	RED	R^b	RED
Water	15.5	16.0	42.3	0	3.022	0	3.007	0	3.381	0	2.955
Ethanol	15.8	8.8	19.4	1	0.951	1	0.972	0	1.298	0	1.221
Acetone	15.5	10.4	7.0	1	0.361	5	0.325	4	0.395	4	0.673
Ethylene glycol	17.0	11.0	26.0	0	1.523	0	1.531	0	1.895	0	1.617
Chloroform	17.8	3.1	5.7	1	0.554	5	0.566	5	0.423	3	0.708
Methylene dichloride	17.0	7.3	7.1	1	0.179	5	0.178	5	0.230	4	0.530
Methyl ethyl ketone	16.0	9.0	5.1	1	0.379	5	0.343	4	0.194	4	0.621
Trichloroethylene	18.0	3.1	5.3	1	0.581	5	0.590	5	0.438	2	0.699
Toluene	18.0	1.4	2.0	1	0.873	4	0.869	5	0.607	1	0.889
Tetrahydrofuran	16.8	5.7	8.0	1	0.246	5	0.277	4	0.316	3	0.646
Ethyl acetate	15.8	5.3	7.2	1	0.372	5	0.390	4	0.290	2	0.777
Dimethyl sulfoxide	18.4	16.4	10.2	1	0.757	2	0.712	0	1.007	5	0.557
Acetonitrile	15.3	18.0	6.1	1	0.932	5	0.874	1	0.988	4	0.887
Dimethyl formamide	17.4	13.7	11.3	1	0.521	5	0.492	3	0.836	4	0.574
Pyridine	19.0	8.8	5.9	1	0.435	3	0.405	5	0.480	3	0.220
Cyclohexane	16.8	0.0	0.2	0	1.055	0	1.048	1	0.731	0	1.111
Benzene	18.4	0.0	2.0	1	0.977	2	0.976	3	0.739	1	0.972
Ethane	15.5	0.0	0.0	0	1.100	0	1.092	1	0.758	0	1.218

[a] Rating for solubility of neat epoxy as the matrix resin.
[b] Rating for the degree of swelling of core/shell nanoparticles.

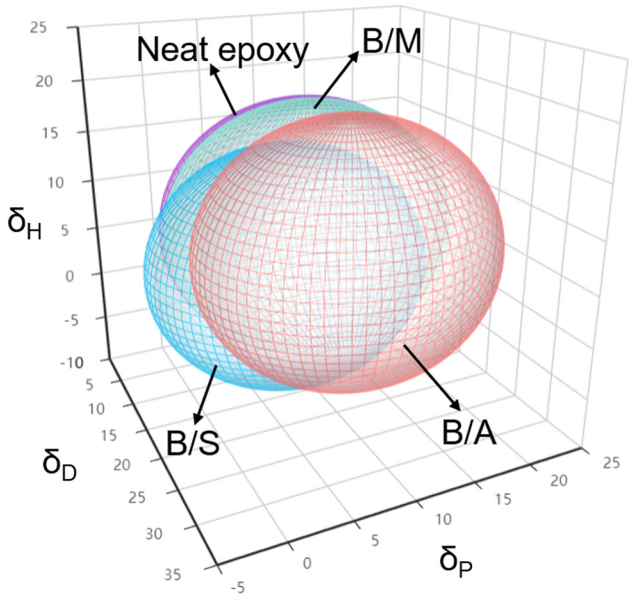

Figure 3: HSP spheres of neat epoxy and core/shell nanoparticles.

presented in Table 2. The solubility parameter components, δ_D, δ_P and δ_H, correspond to the three types of interactions, namely dispersion, polar and hydrogen bond [37,40,41]. The radius R_o of the sphere is the interaction radius. Solvents that fall within R_o are expected to dissolve or swell the corresponding polymer [42]. As shown in Table 2, the δ_D, δ_P and δ_H values for B/S particles were the smallest among the three types of particles, suggesting a weak particle–particle interaction, while the highest values of δ_D and δ_P for B/A particles indicated a strong particle–particle interaction.

Good compatibility generally requires that the respective HSP values for the two polymers are close to each other, thus their R_a, corresponding to the distance between the center of the two polymer spheres, is considered to be a good measure of their compatibility [32,43]. The HSP distance R_a was calculated by the following equation:

$$R_a = (4(\delta_{D1} - \delta_{D2})^2 + (\delta_{P1} - \delta_{P2})^2 + (\delta_{H1} - \delta_{H2})^2)^{1/2}, \quad (1)$$

where subscripts 1 and 2 represent the two different polymers, respectively. In addition, the extent of the overlapping of HSP spheres is an intuitive way to represent compatibility [32]. Therefore, the HSP distance R_a and the overlapping of the spheres were combined to estimate the compatibility between two polymers (Figure 4).

It is evident from Figure 4 that the distance R_a between B/M and the epoxy matrix resin was the smallest (0.50), and the overlapping was the largest. As a matter of fact, the HSP sphere of B/M was completely included in the HSP sphere of the epoxy resin, indicating that the B/M particles had excellent compatibility with the epoxy resin. Differently, the overlap between B/S and the epoxy resin was smaller and the R_a was larger (4.48), so the B/S particles and epoxy resin were less compatible. The R_a of the B/A particles was the largest (6.56), giving the lowest compatibility between B/A and the epoxy resin.

The above analysis demonstrated that the HSP method satisfactorily described and predicted the compatibility and the degree of dispersion of the core/shell particles in the epoxy matrix resin, which agreed with the experimental observations in this study.

Table 2: HSP values for neat epoxy and core/shell nanoparticles

Material	δ_D (MPa$^{1/2}$)	δ_P (MPa$^{1/2}$)	δ_H (MPa$^{1/2}$)	R_o	Data fit
Neat epoxy	17.02	8.34	8.85	11.4	1.000
B/M	17.04	8.83	8.46	11.5	1.000
B/S	16.47	7.03	4.71	11.4	1.000
B/A	19.71	11.14	6.35	12.6	1.000

3.3 Rheological behaviors

The influence of nanofillers on the rheological properties is essentially important for the processing of nanocomposites. Rheology studies provide a convenient way to evaluate the resin–filler interactions, filler–filler interactions, as well as the dispersion of fillers in the resin matrix [44,45]. The shear response is one of the most important characteristics to evaluate the rheological properties. Figure 5 shows the viscosity as a function of shear rate for neat epoxy and epoxy resins containing core/shell nanoparticles. The neat epoxy resin had the lowest viscosity and was mostly Newtonian. As expected, adding nanoparticles increased the viscosity. More specifically, the viscosity of epoxy-B/M and epoxy-B/A increased by about 14 and 17 times, respectively, compared to the neat epoxy. Moreover, adding the B/A particles also made the blend significantly pseudoplastic, *i.e.*, shearing thinning.

Changes in rheological properties when nanoparticles are added to a matrix resin are determined by known factors such as particle morphology and the degree of dispersion, particle–resin and particle–particle interactions. The effect of these factors, however, may not contribute in the same direction or equally. For example, according to the above conclusions, the B/A particles had moderate interaction with the epoxy resin but strong particle–particle attraction due to their high polarity, which formed large aggregates and associative networks

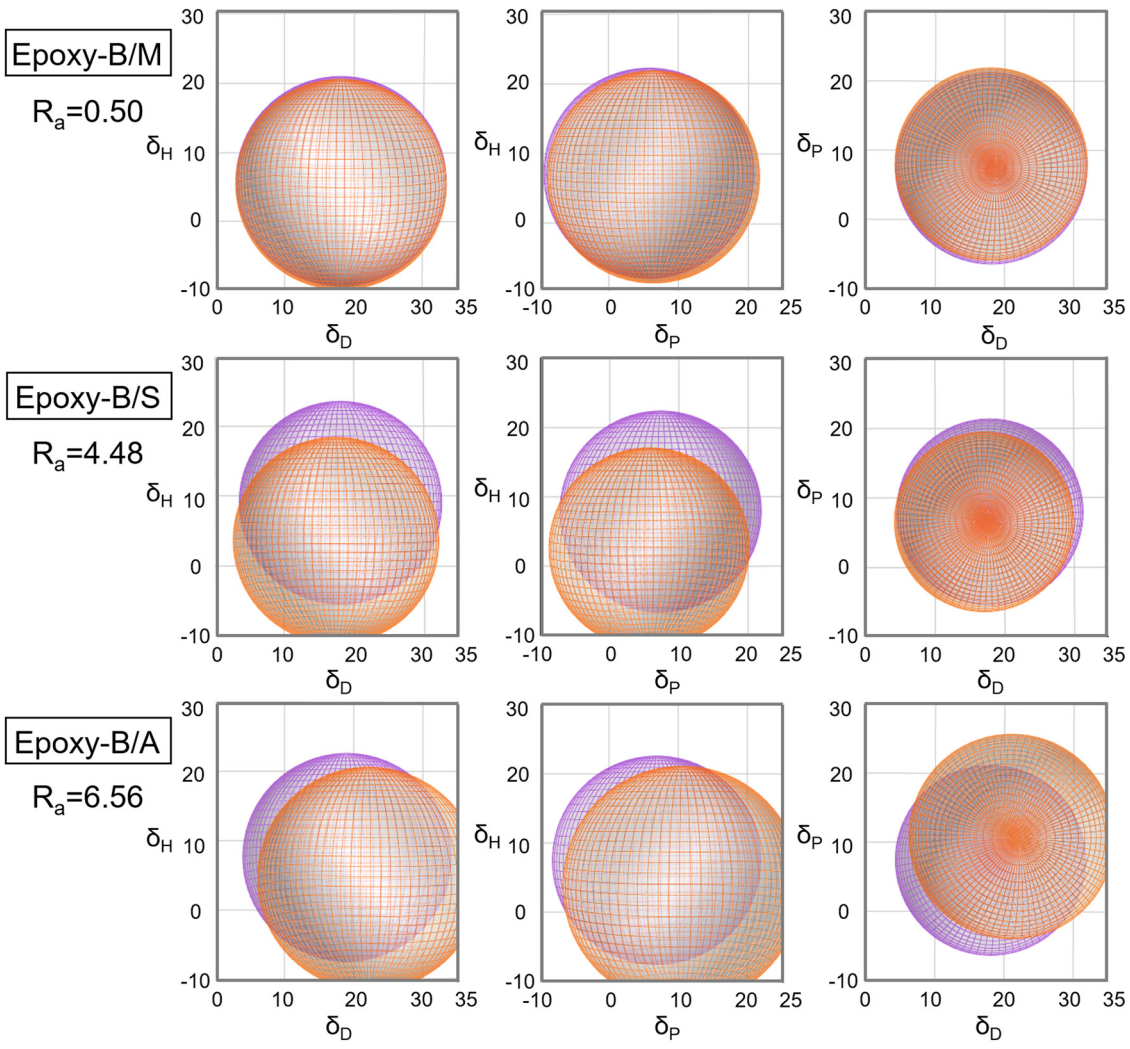

Figure 4: HSP graphs from three-plane projections (front, top and left views). The purple color sphere represents the neat epoxy resin, and the orange color represents core/shell nanoparticles. The R_a values are shown to the left of the HSP graphs.

between particles, leading to high flow resistance, *i.e.*, viscosity. Moreover, these networks of physical association would break apart under high shear, decreasing the viscosity and producing the effect of shear thinning. As for the B/M particles, their good compatibility with epoxy resin meant strong interfacial interaction, consequently inducing a significant increase in the viscosity of the resin mixture. The B/S particles had the least increase in the resin viscosity due to the relatively weak polar force and hydrogen bond in its shell polymer, which led to low particle–particle and epoxy–particle interactions.

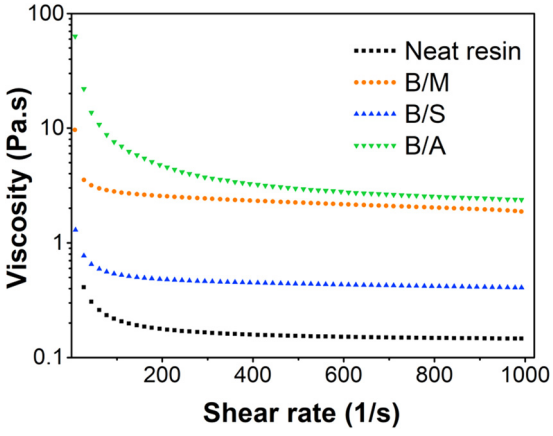

Figure 5: Viscosity *versus* the shear rate of the neat epoxy resin and epoxy resins containing various core/shell nanoparticles.

3.4 Mechanical properties

Literature studies have shown, similarly to the physical properties discussed above, that the nanoparticles'

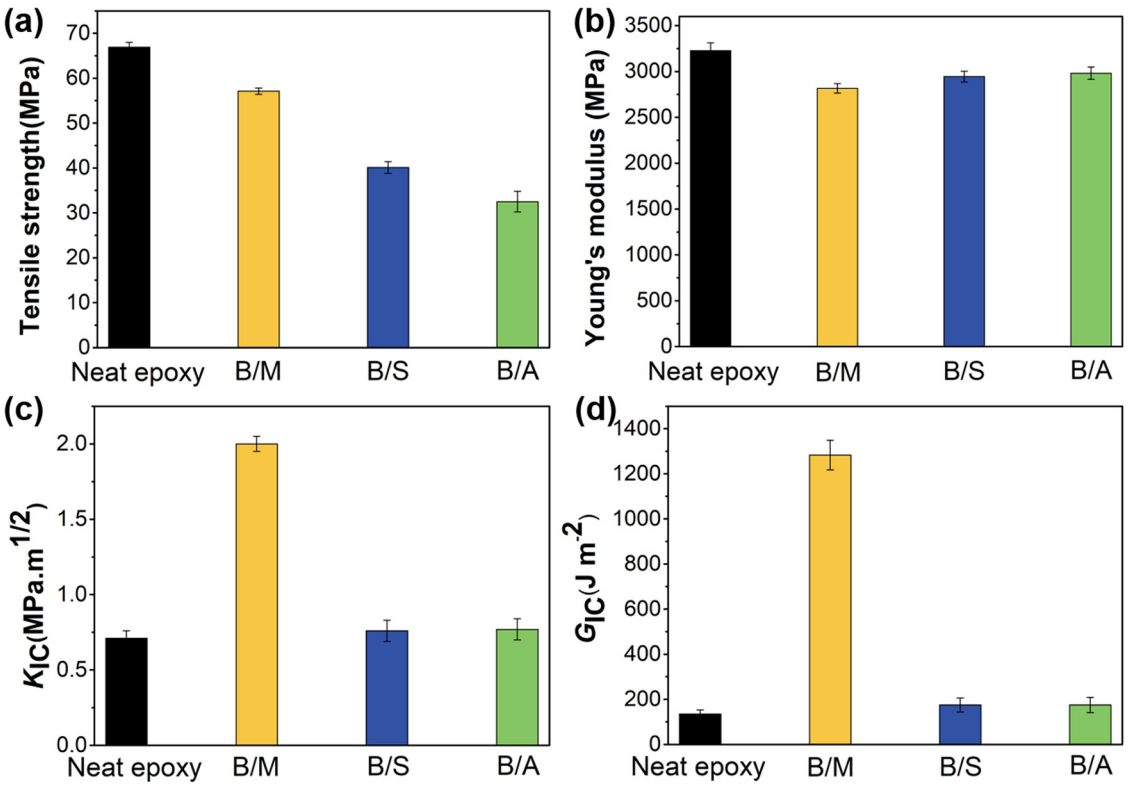

Figure 6: Mechanical properties of neat and nanoparticle-containing epoxy resins: (a) tensile strength, (b) Young's modulus and (c and d) fracture toughness.

degree of dispersion and their interfacial interaction with resins significantly influence the mechanical performance of composite materials *via* load distribution and interfacial stress transfer [30,46]. Based on the above understanding of effects of the shell polymer polarity on the core/shell nanoparticles' dispersion and interfacial interaction, it was expected that the composite mechanical properties would also be a function of the shell composition.

The results of tensile and fracture toughness tests are shown in Figure 6 and the data are summarized in Table S3 (Supplementary Information). Compared to the neat epoxy resin, the tensile strength and Young's modulus of the nanoparticle-containing resins were lower (Figure 6a). More specifically, when B/M, B/S and B/A nanoparticles were incorporated, the tensile strengths decreased by 14.6, 40.0, and 51.4%, respectively. However, their Young's modulus had little changes (Figure 6b). Since tensile strengths are normally controlled by the type and number of defects in the materials and considering that the incorporation of particles introduces a different phase that may act as defects, it would be expected that the tensile strength of the epoxy resin containing particles would decrease. As demonstrated in previous sections, the particle aggregations, both in sizes and severity, were minimal for B/M, but were significant for B/S and the largest for B/A; therefore, the cured resin having the B/A particles would contain the most significant defects and exhibit the highest tensile strength drop, while the resin having B/M particles would show the least strength reduction. Different from the tensile strengths, Young's modulus is determined by the rigidity of the material. With the T_g and the modulus of the shell polymers close to that of the cured epoxy resin, no significant change in the modulus was expected.

As for the effect of core/shell nanoparticles on fracture toughness, which is the main focus of this study, interesting but unsurprising results were observed. It was apparent from Figure 6c and d that only the nanoparticles B/M significantly improved the fracture toughness, with K_{IC} and G_{IC} increasing by 182 and 852%, respectively, compared to the control epoxy resin. This is a higher improvement in toughness than that reported for leading commercial products, *i.e.*, MX125 from Kaneka Corp. gave 127 and 674% gain for K_{IC} and G_{IC}, respectively [47]. Not surprisingly, nanoparticles B/S and B/A showed a little toughening effect.

Again, the root cause for the mechanical property discrepancies was the degree of dispersion of the

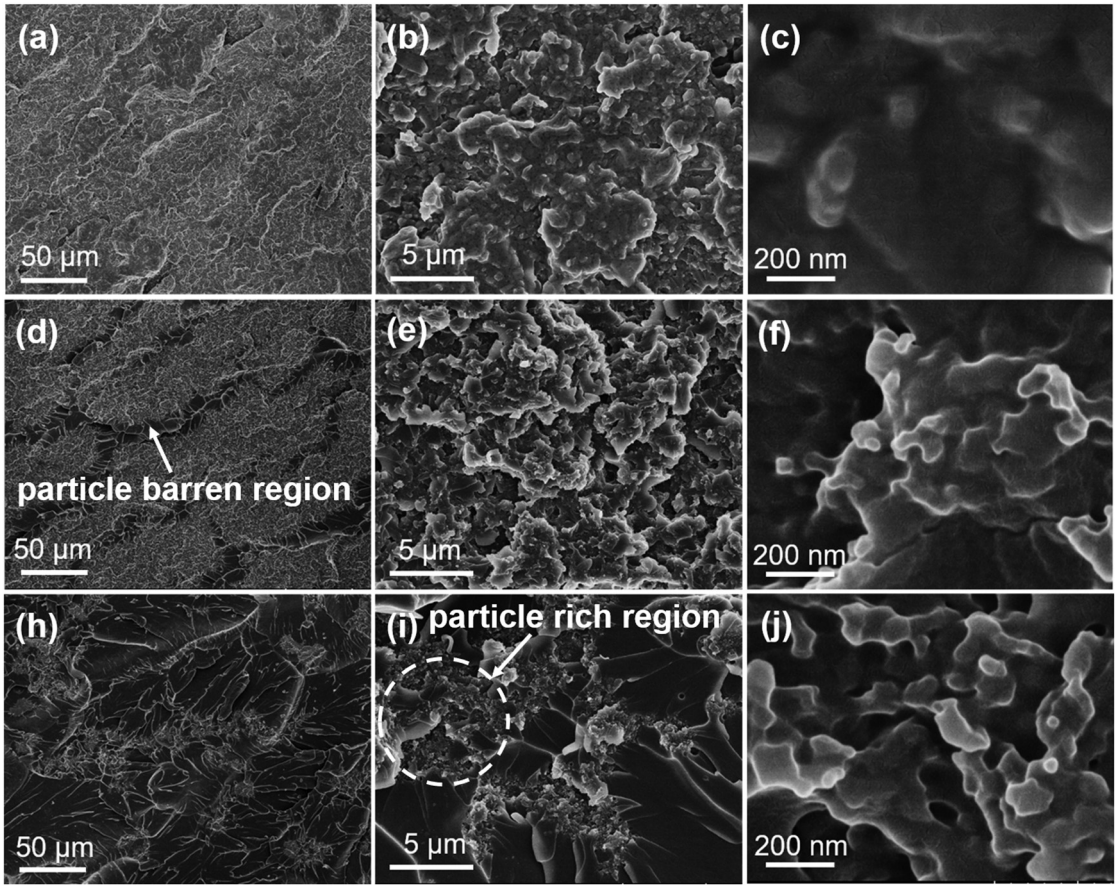

Figure 7: SEM micrographs of fracture surfaces of cured epoxy resins containing particles: (a–c) B/M, (d–f) B/S and (h–j) B/A with the particle-rich region in the focus area.

nanoparticles as observed in the aforementioned TEM, and their compatibility with the epoxy resin as demonstrated by the theory of HSP. In order to further evaluate the effect of the shell polymer polarity on compatibility and interfacial bonding, the fracture surface morphologies were observed by SEM, as shown in Figure 7.

The observation of the fracture surface morphology confirmed the earlier conclusions by TEM. The nanoparticle B/M was uniformly dispersed in the cured epoxy resin, and the fracture surfaces exhibited multiplane features with numerous microcracks, indicating high-energy absorption that was favorable for high fracture toughness. Higher magnification images (Figure 7b–c) revealed that B/M particles were uniformly embedded in the epoxy matrix and no particle pull-out was observed, denoting strong interactions between B/M particles and the resin. In contrast, nanoparticles B/S and B/A both showed aggregations, with a higher level of aggregation for B/A particles than that of B/S particles. The aggregated particles could not effectively block or diffract the crack propagation and absorbed the energy, resulting in no improvement in the toughness. Moreover, it can be observed from Figure 7f and j that a large number of B/S and B/A particles were pulled out from the resin and left empty holes behind them, indicating weak interfacial bonding between particles and the epoxy matrix. These aggregations would readily act as defects that lead to decrease tensile strengths, as observed earlier.

3.5 Modifying nanoparticles under the guidance of HSP theory

The above results demonstrated that the degree of dispersions of the nanoparticles and their interaction with epoxy matrix resin could be well described and predicted by the HSP theory, from which fundamental and reasonable explanations can be derived to describe the physical mechanical behaviors of the particle containing resins. To take this argument further, if the HSP theory truly holds for these nanoparticle-containing epoxy resin

systems, it shall yield predictions on what constitutes the most favorable conditions, as well as points to the direction, toward which modifications could be made to a "bad" particle to turn it into a "good" one. For example, if a particle has a much lower HSP than the resin it intends to toughen, the HSP theory should not only forecast its poor toughening effect but also predict that if the particle's HSP can be increased to match that of the resin's, resulting in higher toughness.

To test the hypothesis, the B/S nanoparticle was selected even though the B/A particle was the lowest performer because the emulsion copolymerization of styrene with a number of co-monomers could be better controlled than that of acrylonitrile. The idea was to use a co-monomer to modify the polarity of the polystyrene shell composition so that it would fall into the solubility parameter ranges calculated from the HSP theory. The degree of dispersion, interfacial interaction and mechanical properties were subsequently studied.

In this study, GMA was selected as the co-monomer, for it carried the more polar epoxy functional groups which happened to be the same as in epoxy resins, and it copolymerized well with styrene. Three levels of GMA were used to copolymerize with styrene and the copolymer became the new shell on the PBA core, producing the modified B/S nanoparticles. The solubility results are presented in Table S4 (Supplementary Information). Table 3 presents the HSP of the modified-B/S nanoparticles. It can be seen from Table 3 that, for the modified B/S particles, their HSP values increases while their HSP distance R_a decreases, with increasing GMA levels, indicating their compatibility with the epoxy resin would become better.

Table 3: Calculated HSP, R_o of B/S, B/S-5, B/S-10 and B/S-15, and HSP distance R_a between these particles and the neat epoxy resin

Material	δ_D ($MPa^{1/2}$)	δ_P ($MPa^{1/2}$)	δ_H ($MPa^{1/2}$)	R_o ($MPa^{1/2}$)	R_a ($MPa^{1/2}$)
B/S	16.47	7.03	4.71	11.4	4.48
B/S-5	16.73	7.71	5.45	11.3	3.51
B/S-10	16.91	8.12	6.69	12.7	2.18
B/S-15	16.84	8.14	7.15	12.5	1.75

Tensile and fracture toughness tests were performed and the results are shown in Figure 8 and Table S3 (Supplementary Information). Compared to the pristine B/S particles, the modified particles produced over 70% increase in tensile strength, reaching the same strength as the neat epoxy resin. More importantly, the modified

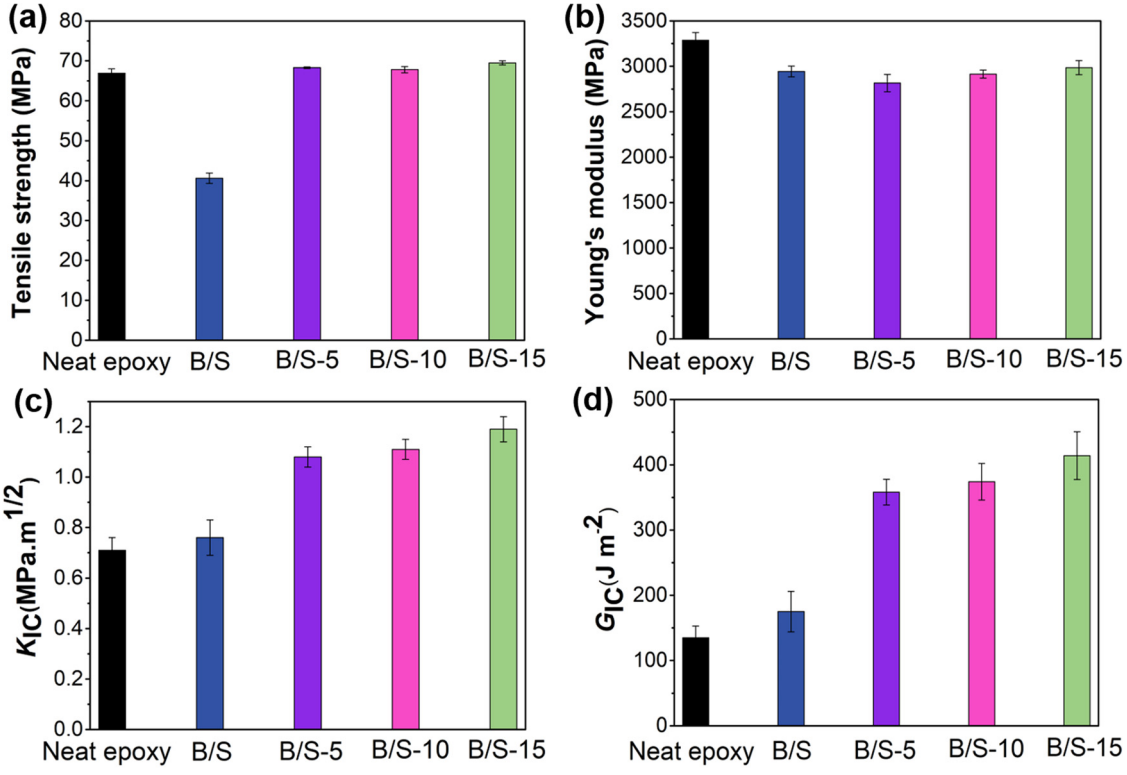

Figure 8: Mechanical properties of cured epoxy resins containing modified particles. Tensile strengths (a), Young's modulus (b) and fracture toughness (c and d).

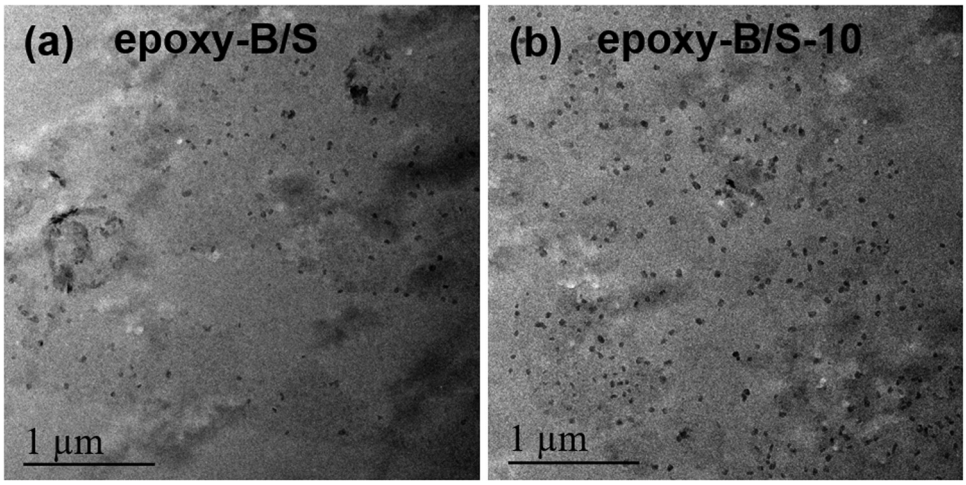

Figure 9: TEM observation of unmodified and GMA-modified B/S particles dispersed in the cured epoxy resin. (a) epoxy-B/S and (b) epoxy-B/S-10.

particles showed significant 46 and 114% increases in K_{IC} and G_{IC}, respectively.

The effect of incorporating GMA on the dispersion state of B/S particles in the epoxy matrix was inspected under a TEM, as shown in Figure 9. It is noted that due to the very close performances of these three modified particles, only the middle-level GMA-modified particle (*i.e.* B/S-10) was selected for the TEM observation. As expected, the GMA-modified-B/S particles showed a much more uniform dispersion in the epoxy matrix, compared to the unmodified particles. To further study the effect of GMA modification on epoxy-particle interaction, the fracture microstructure from the tensile test was examined using an SEM. In the case of unmodified B/S particles (Figure 10a and b), evident particle agglomerates were present and were pulled out of the resin. However, the modified particles in the cured epoxy resin not only exhibited a much more uniform distribution but also showed a much stronger bonding to the resin matrix, as illustrated by Figure 10c and d, which displayed no particle pull-outs.

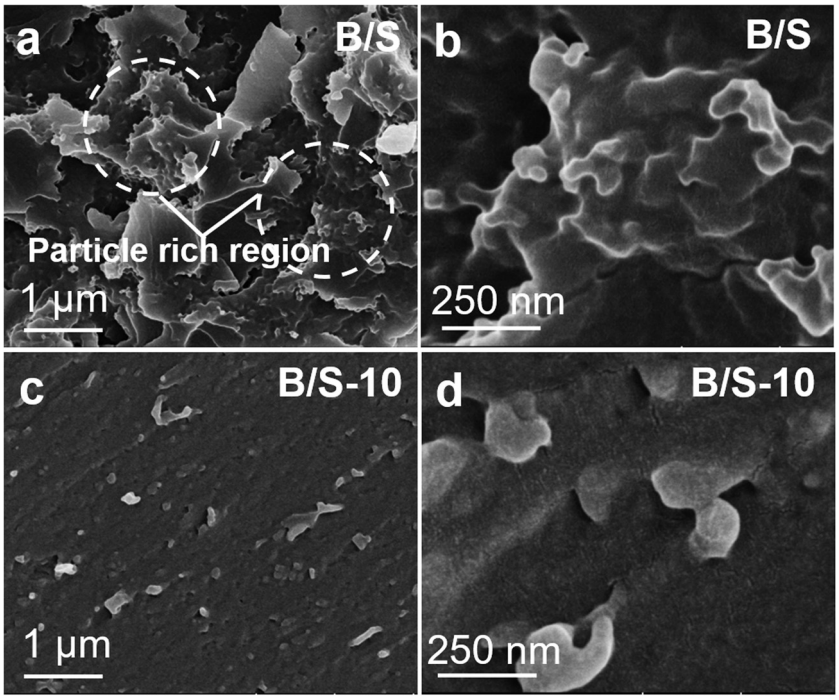

Figure 10: SEM micrographs of fracture surfaces of cured epoxy-B/S (a and b) and epoxy-B/S-10 (c and d) composites after tensile tests.

The above results demonstrated that the HSP theory provides a fundamental understanding and explanation of the physical mechanical performances of polymer composites containing nanoparticles. It further confirms the validity and application of HSP theory as a guide for designing and/or modifying polymer compositions, from which high-performance particles, including but not limited to core/shell nanoparticles, can be synthesized or constructed.

4 Conclusions

This study aimed at understanding the core/shell nanoparticles design principles for epoxy toughening. To achieve this, the composition of core/shell nanoparticles, particularly the shell polymer polarity, was carefully controlled and their effect on the dispersion, rheological and mechanical properties in the epoxy matrix were investigated.

1. The B/M particles, with PMMA as the shell polymer, which had the polarity matching with that of the epoxy matrix resin, would form uniform dispersion, yielding the most significant toughening effect, which was 220 and 851% enhancement in K_{IC} and G_{IC}, respectively.
2. If the polarity of the shell polymer did not match that of the epoxy matrix resin, such as the B/S particles with low shell polymer polarity or the B/A particles with high shell polarity, the particles would more or less aggregate, lowering mechanical performance and leading to little or no toughening.
3. Theoretical HSP compatibility analysis verified that the experimental observations, *i.e.*, the difference in polarity of the shell polymer would greatly affect the compatibility of the core/shell particles with the epoxy matrix, which in turn determined their dispersibility and interfacial interaction.
4. The HSP compatibility not only helped to explain the differences in particle toughening performances but also facilitated the design of better core/shell nanoparticles for effective epoxy toughening.

Acknowledgements: The authors are grateful for the reviewer's valuable comments that improved the manuscript.

Funding information: The authors state no funding involved.

Author contributions: All authors have accepted responsibility for the entire content of this manuscript and approved its submission.

Conflict of interest: The authors state no conflict of interest.

Data availability statement: All data generated or analysed during this study are included in this published article and its supplementary information files.

References

[1] Park YT, Qian Y, Chan C, Suh T, Nejhad MG, Macosko CW, et al. Epoxy toughening with low graphene loading. Adv Funct Mater. 2015;25(4):575–85.
[2] Zhou S, Chen Z, Tusiime R, Cheng C, Sun Z, Xu L, et al. Highly improving the mechanical and thermal properties of epoxy resin via blending with polyetherketone cardo. Compos Commun. 2019;13:80–4.
[3] Chen Z, Luo J, Huang Z, Cai C, Tusiime R, Li Z, et al. Synergistic toughen epoxy resin by incorporation of polyetherimide and amino groups grafted MWCNTs. Compos Commun. 2020;21:100377.
[4] Mehrabi-Kooshki M, Jalali-Arani A. Preparation of binary and hybrid epoxy nanocomposites containing graphene oxide and rubber nanoparticles: Fracture toughness and mechanical properties. J Appl Polym Sci. 2019;136(4):1–9.
[5] Rodríguez ES, Falchi VG, Asaro L, Zucchi IA, Williams RJJ. Toughening an epoxy network by the addition of an acrylic triblock copolymer and halloysite nanotubes. Compos Commun. 2019;12:86–90.
[6] Padinjakkara A, Salim N, Thomas S. Effect of hexamethyldisilazane-modified nano fumed silica on the properties of epoxy/carboxyl-terminated poly(butadiene-co-acrylonitrile) blend: a new hybrid approach. Ind Eng Chem Res. 2020;59(7):2883–91.
[7] Chen H, Lian Q, Xu W, Hou X, Li Y, Wang Z, et al. Insights into the synergistic mechanism of reactive aliphatic soft chains and nano-silica on toughening epoxy resins with improved mechanical properties and low viscosity. J Appl Polym Sci. 2021;138(21):1–11.
[8] Jiang T, Ren X, Tu Z, Shi H, Wang J, Hu G-H, et al. Critical rubber layer thickness of core-shell particles with a rigid core and a soft shell for toughening of epoxy resins without loss of elastic modulus and strength. Compos Sci Technol. 2017;153:253–60.
[9] Quan D, Ivankovic A. Effect of core-shell rubber (CSR) nanoparticles on mechanical properties and fracture toughness of an epoxy polymer. Polymer. 2015;66:16–28.
[10] Wang J, Xue Z, Li Y, Li G, Wang Y, Zhong WH, et al. Synergistically effects of copolymer and core-shell particles for toughening epoxy. Polymer. 2018;140:39–46.
[11] Mirzaee R, Aref-Azar A. Modeling and optimizing toughness and rigidity of PA6/SBR: Using compatibilizer and response surface methodology. Polym Test. 2020;83:106346.
[12] Odrobina M, Deák T, Székely L, Mankovits T, Keresztes RZ, Kalácska G. The effect of crystallinity on the toughness of cast polyamide 6 rods with different diameters. Polymers. 2020;12(2):293.
[13] Deng H, Yuan L, Gu A, Liang G. Facile strategy and mechanism of greatly toughening epoxy resin using polyethersulfone through

controlling phase separation with microwave-assisted thermal curing technique. J Appl Polym Sci. 2020;137(8):1–12.
[14] Kou Y, Zhou W, Li B, Dong L, Duan YE, Hou Q, et al. Enhanced mechanical and dielectric properties of an epoxy resin modified with hydroxyl-terminated polybutadiene. Compos Part A Appl Sci Manuf. 2018;114:97–106.
[15] Wang Y, Chen S, Chen X, Lu Y, Miao M, Zhang D. Controllability of epoxy equivalent weight and performance of hyperbranched epoxy resins. Compos Part B Eng. 2019;160:615–25.
[16] Ricciardi MR, Papa I, Langella A, Langella T, Lopresto V, Antonucci V. Mechanical properties of glass fibre composites based on nitrile rubber toughened modified epoxy resin. Compos Part B Eng. 2018;139:259–67.
[17] Tian Y, Zhang H, Zhang Z. Influence of nanoparticles on the interfacial properties of fiber-reinforced-epoxy composites. Compos Part A Appl Sci Manuf. 2017;98:1–8.
[18] Roy S, Petrova RS, Mitra S. Effect of carbon nanotube (CNT) functionalization in epoxy-CNT composites. Nanotechnol Rev. 2018;7(6):475–85.
[19] Chen J, Yan L, Song W, Xu D. Interfacial characteristics of carbon nanotube-polymer composites: a review. Compos Part A Appl Sci Manuf. 2018;114:149–69.
[20] Zhang H, Li X, Qian W, Zhu J, Chen B, Yang J, et al. Characterization of mechanical properties of epoxy/nanohybrid composites by nanoindentation. Nanotechnol Rev. 2020;9(1):28–40.
[21] Ladani RB, Wu S, Kinloch AJ, Ghorbani K, Zhang J, Mouritz AP, et al. Improving the toughness and electrical conductivity of epoxy nanocomposites by using aligned carbon nanofibres. Compos Sci Technol. 2015;117:146–58.
[22] Xu Z, Song P, Zhang J, Guo Q, Mai YW. Epoxy nanocomposites simultaneously strengthened and toughened by hybridization with graphene oxide and block ionomer. Compos Sci Technol. 2018;168(10):363–70.
[23] Wu Y, Tang B, Liu K, Zeng X, Lu J, Zhang T, et al. Enhanced flexural properties of aramid fiber/epoxy composites by graphene oxide. Nanotechnol Rev. 2019;8(1):484–92.
[24] Tang LC, Zhang H, Sprenger S, Ye L, Zhang Z. Fracture mechanisms of epoxy-based ternary composites filled with rigid-soft particles. Compos Sci Technol. 2012;72(5):558–65.
[25] Nguyen TKL, Soares BG, Duchet-Rumeau J, Livi S. Dual functions of ILs in the core-shell particle reinforced epoxy networks: curing agent vs dispersion aids. Compos Sci Technol. 2017;140:30–8.
[26] Ning N, Liu W, Hu Q, Zhang L, Jiang Q, Qiu Y, et al. Impressive epoxy toughening by a structure-engineered core/shell polymer nanoparticle. Compos Sci Technol. 2020;199.
[27] Li W, Shang T, Yang W, Yang H, Lin S, Jia X, et al. Effectively exerting the reinforcement of dopamine reduced graphene oxide on epoxy-based composites via strengthened interfacial bonding. ACS Appl Mater Interfaces. 2016;8(20):13037–50.
[28] Vijayan PP, Pionteck J, Huczko A, Puglia D, Kenny JM, Thomas S. Liquid rubber and silicon carbide nanofiber modified epoxy nanocomposites: Volume shrinkage, cure kinetics and properties. Compos Sci Technol. 2014;102:65–73.
[29] Liu Y, Jiang X, Shi J, Luo Y, Tang Y, Wu Q, et al. Research on the interface properties and strengthening-toughening mechanism of nanocarbon-toughened ceramic matrix composites. Nanotechnol Rev. 2020;9(1):190–208.
[30] Liu W, Wang Y, Wang P, Li Y, Jiang Q, Hu X, et al. A biomimetic approach to improve the dispersibility, interfacial interactions and toughening effects of carbon nanofibers in epoxy composites. Compos Part B Eng. 2017;113:197–205.
[31] Wang G, Dai Z, Liu L, Hu H, Dai Q, Zhang Z. Tuning the interfacial mechanical behaviors of monolayer graphene/PMMA nanocomposites. ACS Appl Mater Interfaces. 2016;8(34):22554–62.
[32] Ma J, Larsen RM. Comparative study on dispersion and interfacial properties of single walled carbon nanotube/polymer composites using Hansen solubility parameters. ACS Appl Mater Interfaces. 2013;1293(1):1287–93.
[33] Blond D, Barron V, Ruether M, Ryan KP, Nicolosi V, Blau WJ, et al. Enhancement of modulus, strength, and toughness in poly(methyl methacrylate)-based composites by the incorporation of poly(methyl methacrylate)-functionalized nanotubes. Adv Funct Mater. 2006;16(12):1608–14.
[34] Jeon GG, Lee M, Nam J, Park W, Yang M, Choi J, et al. Simple solvent engineering for high-mobility and thermally robust conjugated polymer nanowire field-effect transistors. ACS Appl Mater Interfaces. 2018;10(35):29824–30.
[35] Van Krevelen DW, Te Nijenhuis K. Properties of polymers: their correlation with chemical structure; their numerical estimation and prediction from additive group contributions. UK: Elsevier; 2009.
[36] Imbrogno J, Williams MD, Belfort G. A new combinatorial method for synthesizing, screening, and discovering antifouling surface chemistries. ACS Appl Mater Interfaces. 2015;7(4):2385–92.
[37] Hansen CM. Hansen Solubility Parameters. Boca Raton: CRC Press; 2007. p. 544.
[38] Jang BN, Wang D, Wilkie CA. Relationship between the solubility parameter of polymers and the clay dispersion in polymer/clay nanocomposites and the role of the surfactant. Macromolecules. 2005;38(15):6533–43.
[39] Milliman HW, Boris D, Schiraldi DA. Experimental determination of Hansen solubility parameters for select POSS and polymer compounds as a guide to POSS-polymer interaction potentials. Macromolecules. 2012;45(4):1931–6.
[40] Chang M, Choi D, Fu B, Reichmanis E. Solvent based hydrogen bonding: Impact on poly(3-hexylthiophene) nanoscale morphology and charge transport characteristics. ACS Nano. 2013;7(6):5402–13.
[41] Bergin SD, Sun Z, Rickard D, Streich P V, Hamilton JP, Coleman JN. Multicomponent solubility parameters for single-walled carbon nanotube-solvent mixtures. ACS Nano. 2009;3(8):2340–50.
[42] Takeuchi KJ, Takeuchi ES, Reichmanis E. Toward uniformly dispersed battery electrode composite materials: Characteristics and performance. ACS Appl Mater Interfaces. 2016;8(5):3452–63.
[43] Hansen CM. Polymer additives and solubility parameters. Prog Org Coatings. 2004;51(5):109–12.
[44] Krishnamoorti R, Ren J, Silva AS. Shear response of layered silicate nanocomposites. J Chem Phys. 2001;114(11):4968–73.
[45] Zhu J, Wei S, Ryu J, Budhathoki M, Liang G, Guo Z. In situ stabilized carbon nanofiber (CNF) reinforced epoxy nanocomposites. J Mater Chem. 2010;20(23):4937–48.
[46] Yang L, Phua SL, Kai J, Teo H, Toh CL, Lau SK, et al. A biomimetic approach to enhancing interfacial interactions: polydopamine-coated clay as reinforcement for epoxy resin. ACS Appl Mater Interfaces. 2011;3(8):3026–32.
[47] Giannakopoulos G, Masania K, Taylor AC. Toughening of epoxy using core-shell particles. J Mater Sci. 2011;46(2):327–38.